RESEARCH BRIEF

Clinical Acquired Resistance to KRAS^{G12C} Inhibition through a Novel KRAS Switch-II Pocket Mutation and Polyclonal Alterations Converging on RAS–MAPK Reactivation

Noritaka Tanaka[1], Jessica J. Lin[1], Chendi Li[1], Meagan B. Ryan[1], Junbing Zhang[1], Lesli A. Kiedrowski[2], Alexa G. Michel[1], Mohammed U. Syed[1], Katerina A. Fella[1], Mustafa Sakhi[1], Islam Baiev[1], Dejan Juric[1], Justin F. Gainor[1], Samuel J. Klempner[1], Jochen K. Lennerz[3], Giulia Siravegna[1], Liron Bar-Peled[1], Aaron N. Hata[1], Rebecca S. Heist[1], and Ryan B. Corcoran[1]

ABSTRACT

Mutant-selective KRAS^{G12C} inhibitors, such as MRTX849 (adagrasib) and AMG 510 (sotorasib), have demonstrated efficacy in *KRAS*^{G12C}-mutant cancers, including non–small cell lung cancer (NSCLC). However, mechanisms underlying clinical acquired resistance to KRAS^{G12C} inhibitors remain undetermined. To begin to define the mechanistic spectrum of acquired resistance, we describe a patient with *KRAS*^{G12C} NSCLC who developed polyclonal acquired resistance to MRTX849 with the emergence of 10 heterogeneous resistance alterations in serial cell-free DNA spanning four genes (*KRAS, NRAS, BRAF, MAP2K1*), all of which converge to reactivate RAS–MAPK signaling. Notably, a novel *KRAS*^{Y96D} mutation affecting the switch-II pocket, to which MRTX849 and other inactive-state inhibitors bind, was identified that interferes with key protein–drug interactions and confers resistance to these inhibitors in engineered and patient-derived *KRAS*^{G12C} cancer models. Interestingly, a novel, functionally distinct tricomplex KRAS^{G12C} active-state inhibitor RM-018 retained the ability to bind and inhibit KRAS$^{G12C/Y96D}$ and could overcome resistance.

SIGNIFICANCE: In one of the first reports of clinical acquired resistance to KRAS^{G12C} inhibitors, our data suggest polyclonal RAS–MAPK reactivation as a central resistance mechanism. We also identify a novel KRAS switch-II pocket mutation that impairs binding and drives resistance to inactive-state inhibitors but is surmountable by a functionally distinct KRAS^{G12C} inhibitor.

See related commentary by Pinnelli and Trusolino, p. 1874.

INTRODUCTION

The development of compounds that bind covalently to cysteine 12 in KRAS^{G12C} cancers has ushered in a new era in efforts to target KRAS directly. Biochemically, these agents lock KRAS in its inactive GDP-bound conformation, thereby inhibiting downstream signaling, leading to preclinical antitumor responses (1–3). The lead clinical compounds sotorasib (AMG 510) and adagrasib (MRTX849) have advanced rapidly and demonstrated tolerability and single-agent activity across *KRAS*^{G12C}-mutant cancers (4, 5). In patients with advanced non–small cell lung cancer (NSCLC) harboring KRAS^{G12C} (which comprises approximately 13% of all lung adenocarcinomas), AMG 510 and MRTX849 have

[1]Massachusetts General Hospital Cancer Center and Department of Medicine, Harvard Medical School, Boston, Massachusetts. [2]Guardant Health, Redwood City, California. [3]Department of Pathology, Massachusetts General Hospital, Boston, Massachusetts.

Note: Supplementary data for this article are available at Cancer Discovery Online (http://cancerdiscovery.aacrjournals.org/).

N. Tanaka, J.J. Lin, and C. Li contributed equally to this work.

Corresponding Authors: Aaron N. Hata, Massachusetts General Hospital Cancer Center, 149 13th Street, 7th Floor, Boston, MA 02129. Phone: 617-724-3442; E-mail: ahata@mgh.harvard.edu; Rebecca S. Heist, Massachusetts General Hospital Cancer Center, 55 Fruit Street, Boston, MA 02114. Phone: 617-724-4000; E-mail: rheist@partners.org; and Ryan B. Corcoran, Massachusetts General Hospital Cancer Center, 149 13th Street, 7th Floor, Boston, MA 02129. Phone: 617-726-8599; E-mail: rbcorcoran@partners.org

Cancer Discov 2021;11:1913–22

doi: 10.1158/2159-8290.CD-21-0365

demonstrated meaningful efficacy with objective response rates of 37% and 45%, as well as disease control rates of 81% and 96%, respectively (6, 7). AMG 510 has recently received Breakthrough Therapy designation from the FDA for the treatment of patients with advanced *KRAS*^{G12C}-mutant NSCLC following at least one prior systemic therapy. Multiple ongoing trials seek to augment responses to KRAS^{G12C} inhibitors through combination strategies.

Preclinical studies with MRTX849 and other KRAS^{G12C} inhibitors have suggested several mechanisms of up-front resistance, including reactivation of ERK-dependent signaling to bypass KRAS^{G12C} blockade (4). Prior work by our group and others has identified adaptive RAS pathway feedback reactivation as a key mechanism of primary resistance to KRAS^{G12C} inhibition (8–13). However, the key mechanisms of clinical acquired resistance to KRAS^{G12C} inhibitors are currently unknown. Here, as an initial effort to characterize the clinical landscape of potential acquired resistance mechanisms to KRAS^{G12C} inhibitors, we present a patient with *KRAS*^{G12C}-mutant NSCLC who developed acquired resistance to MRTX849, characterized by the emergence of 10 individual resistance alterations involving four RAS–MAPK genes. All of these resistance alterations converge to reactivate RAS–MAPK signaling, implicating this as a potential central mechanism of acquired resistance. We also identify a novel *KRAS*^{Y96D} resistance mutation in the switch-II pocket of KRAS through serial cell-free DNA (cfDNA) analysis. Through structural modeling and *in vitro* functional studies, we find that KRAS^{Y96D} confers resistance to multiple KRAS^{G12C} inhibitors currently in clinical development but identify a novel active-state KRAS^{G12C} inhibitor, RM-018, that is able to overcome KRAS$^{G12C/Y96D}$-mediated resistance.

RESULTS

Heterogeneous Acquired Resistance Alterations Converge on RAS–MAPK Reactivation

A 67-year-old woman with metastatic *KRAS*^{G12C}-mutant NSCLC was treated on the dose-expansion cohort of the phase 1 study of MRTX849 (NCT03785249; Methods; further detailed in Supplementary Methods). Initial scans showed a 32% reduction in tumor size (by RECIST v1.1), but after approximately 4 months of treatment, the patient developed progressive disease, and the patient discontinued therapy at 5.5 months (Fig. 1A). To identify putative mechanisms of acquired resistance to MRTX849 in this patient, we assessed cfDNA using a targeted next-generation sequencing assay (Guardant360; Guardant Health) and droplet digital PCR (ddPCR). Upon development of acquired resistance, the original *KRAS*^{G12C} and *TP53*^{F338fs} variants present in pretreatment tumor and cfDNA were again detected in cfDNA but were accompanied by the emergence of 10 distinct mutations affecting RAS–MAPK components *KRAS, NRAS, BRAF*, and *MAP2K1* (which encodes the MEK1 protein) identified across cfDNA specimens obtained after disease progression (Fig. 1B; Supplementary Table S1). The lower allele frequencies of these alterations relative to the truncal *KRAS*^{G12C} and *TP53* mutations are consistent with the emergence of these mutations in heterogeneous subclonal populations. These included three activating *NRAS* mutations (*NRAS*^{Q61L}, *NRAS*^{Q61K}, *NRAS*^{Q61R}), which can drive active RAS signaling in a KRAS-independent manner, and *BRAF*^{V600E}, which can maintain MAPK signaling downstream of KRAS^{G12C} in the presence of MRTX849 (Supplementary Fig. S1). Three *MAP2K1* mutations (*MAP2K1*^{K57N}, *MAP2K1*^{Q56P}, *MAP2K1*$^{E102\text{-}I103del}$) previously demonstrated to be activating and known to be involved in resistance to upstream MAPK pathway inhibitors (i.e., BRAF inhibitors) were also identified (14, 15).

In addition, three *KRAS* mutations emerged in the postprogression cfDNA. Two of these mutations are the known activating mutations *KRAS*^{G13D} and *KRAS*^{G12V}, and mutant-selective KRAS^{G12C} inhibitors have previously been shown to be ineffective against these mutations (4, 16). A deeper analysis of individual sequencing reads from cfDNA suggested that these mutations seemed to occur in *trans* to the original *KRAS*^{G12C} mutation (Supplementary Fig. S2A and S2B), likely arising in the remaining wild-type copy of *KRAS*, which appeared to be retained based on pretreatment tumor sequencing (Supplementary Table S2). However, it is not possible from the cfDNA data to confirm that these mutations coexist in cells that also harbor the original *KRAS*^{G12C} mutation. Notably, a single, well-supported family of sequencing reads from the same original template molecule showed the concurrent presence of both nucleotide changes corresponding to *KRAS*^{G12C} and *KRAS*^{G12V} in *cis* on the same strand, which would encode for a *KRAS*^{G12F} mutation. While it is not possible to confirm the presence of this mutation based on a single read family, this finding raises the possibility that *cis* mutations resulting in "loss" of the original *KRAS*^{G12C} mutation and conversion to a different *KRAS* mutation might be another potential mechanism of resistance. Notably, all putative resistance mutations identified are predicted to converge on reactivation of RAS–MAPK pathway signaling, suggesting that this may represent a common primary mechanism of acquired resistance to KRAS^{G12C} inhibitors (Fig. 1C).

Interestingly, the third *KRAS* mutation identified, *KRAS*^{Y96D}, represents a novel mutation that is not known to be activating. Notably, although *KRAS* is the most commonly mutated oncogene in human cancer, a search of two large tumor mutational databases—COSMIC and GENIE, which collectively contain >450,000 molecularly characterized cancers (17, 18)—did not reveal a single previously identified mutation at the *KRAS*^{Y96} locus among >75,000 cases with documented *KRAS* mutations (Supplementary Table S3). However, the Y96 residue is associated with the switch-II pocket to which MRTX849 and other inactive-state KRAS^{G12C} inhibitors bind, suggesting that the previously undescribed Y96D mutation may have a novel and specific role in driving resistance to KRAS^{G12C} inhibitors.

Structural Modeling of KRAS$^{G12C/Y96D}$

To understand the significance of the acquired *KRAS*^{Y96D} mutation, we performed structural modeling of the G12C-mutant and G12C/Y96D double-mutant KRAS proteins bound to the KRAS^{G12C} inhibitors MRTX849, AMG 510, and ARS-1620 (Fig. 2). These three inhibitors bind the GDP state of KRAS^{G12C} and exploit a cryptic pocket formed by the central β sheet of RAS and switch-II (first identified by Ostrem and

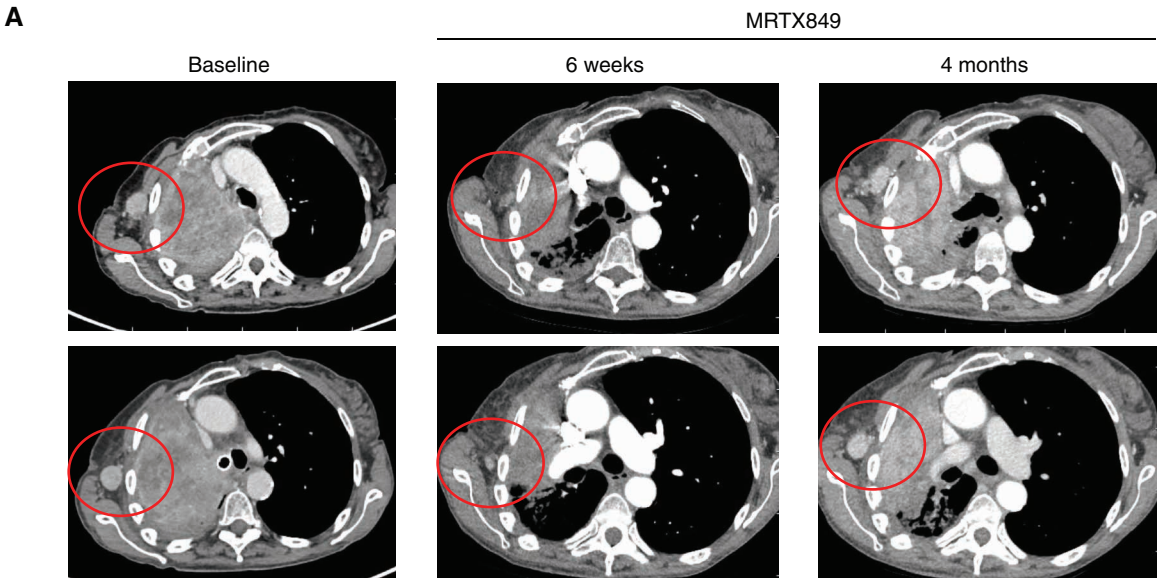

B

	Tumor	cfDNA			
	Pre-MRTX849	Pre-MRTX849	Days post-MRTX849 discontinuation: 0	9	51
TP53 F338fs	36.8%	0.22%	8.8%	10.1%	14.3%
KRAS G12C	21.3%	0.12%	31.7%	47.1%	24.9%
KRAS G12V	-	-	-	-	0.09%
KRAS G13D	-	-	-	0.13%†	0.04%
KRAS Y96D	-	-	0.4%	0.2%	-
NRAS Q61L	-	-	-	0.2%	-
NRAS Q61R	-	-	-	-	0.02%
NRAS Q61K	-	-	0.6%	0.6%	0.9%
BRAF V600E	-	-	0.1%	0.1%	0.5%
MAP2K1 K57N	-	-	0.05%†	-	0.3%
MAP2K1 Q56P	-	-	-	-	0.1%
MAP2K1 E102_I103del	-	-	-	0.12%†	0.2%

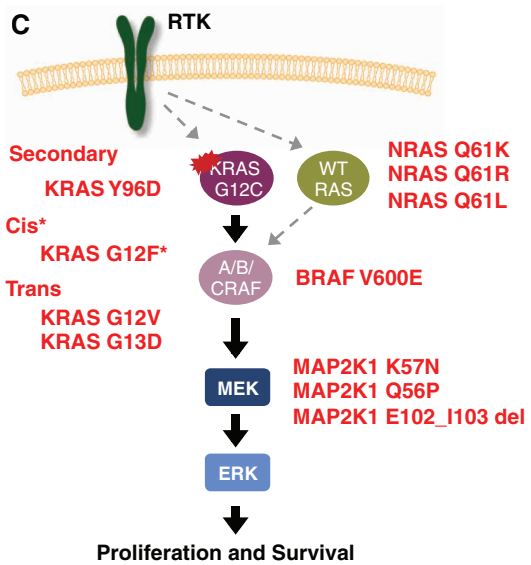

Figure 1. Acquired resistance to KRAS^{G12C} inhibitor MRTX849 (adagrasib). **A,** Computed tomography images of the patient's axillary lymph node metastasis at baseline, during response to MRTX849, and at progression on MRTX849. **B,** Variant allele fractions of mutations detected in the patient's serial plasma samples. †, indicates the mutations were detected by ddPCR but not by plasma next-generation sequencing. **C,** Alterations detected in post-MRTX849 cfDNA include acquired mutations in *KRAS* as well as multiple components of the MAPK signaling cascade. *, KRAS^{G12F} represents a potential resistance mechanism supported by limited sequencing reads, as shown in Supplementary Fig. S2.

colleagues; ref. 3). To determine the effects of the amino acid substitution at the Y96 locus, crystal structures of MRTX849, AMG 510, and ARS-1620 bound to KRAS^{G12C} were modeled for interactions with the Y96 residue within the switch-II pocket (16, 19–21). The hydroxyl group of Y96 forms a direct hydrogen bond with the pyrimidine ring of MTRX849, which is abolished with the Y96D mutation. Y96D also disrupts the water-mediated hydrogen bond between Y96 and a carboxyl group on AMG 510. Finally, although Y96 does not form a direct hydrogen bond with ARS-1620, it stabilizes the interaction with ARS-1620 through pi-stacking with the phenyl ring of Y96, which is disrupted with the Y96D mutation. In addition, by introducing a negatively charged amino acid, the Y96D mutation changes the hydrophobic nature of the binding pocket for all three compounds to a substantially more hydrophilic pocket, which may further destabilize binding.

Functional Characterization of KRAS^{Y96D}

To assess whether KRAS^{Y96D} can mediate resistance to MRTX849 and other inactive-state KRAS^{G12C} inhibitors, we expressed KRAS^{G12C} or the KRAS$^{G12C/Y96D}$ double mutant in NCI-H358 (*KRAS*^{G12C}-mutant NSCLC), MIA PaCa-2

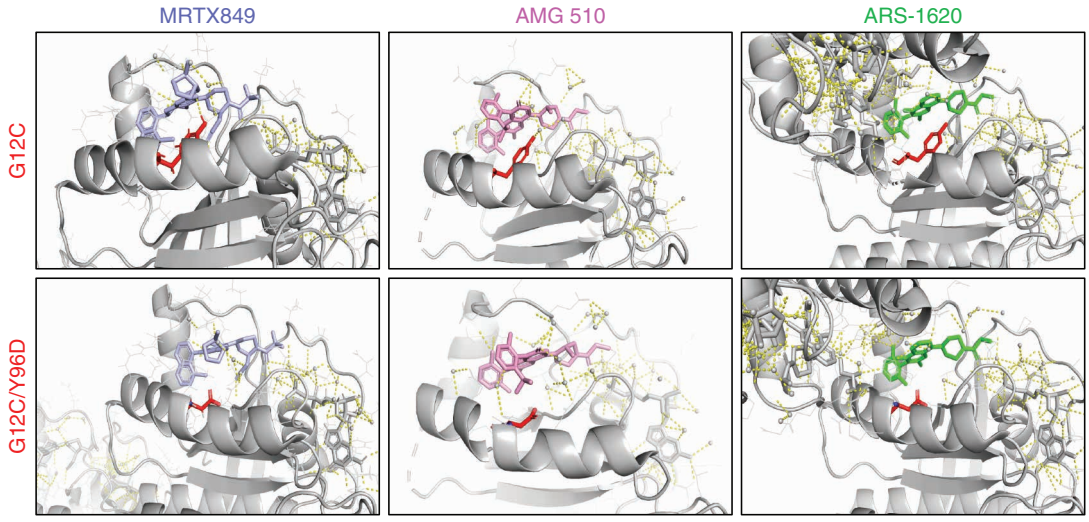

Figure 2. Structural basis for resistance to KRAS^{G12C} inhibition conferred by KRAS^{Y96D}. Shown are the modeled crystal structures of MRTX849 (6UT0), AMG 510 (6OIM), and ARS-1620 (5V9U) bound to KRAS^{G12C} (top) and KRAS$^{G12C/Y96D}$ (bottom), highlighting the loss of the hydrogen bonds between MRTX849 or AMG 510 and the Y96 residue and the disruption of the switch-II pocket dynamics between ARS-1620 and KRAS$^{G12C/Y96D}$.

(*KRAS*^{G12C}-mutant pancreatic ductal adenocarcinoma), and Ba/F3 cells, which lack endogenous KRAS^{G12C} but become oncogene dependent upon withdrawal of IL3. In cell viability assays, relative to KRAS^{G12C}-expressing controls, cells expressing KRAS$^{G12C/Y96D}$ showed marked resistance to three KRAS^{G12C} inhibitors, with IC_{50} shifts of >100-fold for MRTX849 and AMG 510 and ~20-fold for ARS-1620 (Fig. 3A; Supplementary Table S4).

Consistent with the effects on cell viability, RAS–MAPK pathway activity, as measured by levels of phosphorylated ERK (pERK) and pRSK, was sustained in KRAS$^{G12C/Y96D}$-expressing MIA PaCa-2 cells even at high concentrations of MRTX849, relative to cells expressing KRAS^{G12C} alone (Fig. 3B). Similarly, in *KRAS*^{G12C}-mutant NSCLC cells in which PI3K signaling is driven by mutant KRAS, including an existing patient-derived model MGH1138-1, persistent pERK and pAKT levels were observed with KRAS$^{G12C/Y96D}$ in the presence of MRTX849, relative to KRAS^{G12C} expression alone (Fig. 3C; Supplementary Fig. S3). KRAS$^{G12C/Y96D}$ also drove marked resistance to MRTX849 in the patient-derived MGH1138-1 model. Furthermore, in 293T cells, which lack endogenous KRAS^{G12C} expression, MRTX849 was unable to inhibit pERK levels driven by KRAS$^{G12C/Y96D}$ (Fig. 3D). Because MRTX849 and other inactive-state KRAS^{G12C} inhibitors bind covalently to KRAS^{G12C}, an electrophoretic mobility shift of drug-adducted KRAS^{G12C} can be observed upon drug binding due to increased molecular weight. However, this mobility shift was no longer observed when 293T cells expressing KRAS$^{G12C/Y96D}$ were treated with MRTX849, suggesting that the Y96D mutation may abrogate inhibitor binding. Notably, KRAS$^{G12C/Y96D}$ appeared to have higher basal activation than KRAS^{G12C}, as measured by a higher proportion of the active GTP-bound form of KRAS, although activation still appeared to be partly dependent on upstream pathway input (Supplementary Fig. S4A and S4B). Finally, although a decrease in GTP-bound KRAS (representing the active state) was observed in KRAS^{G12C}-expressing cells treated with MRTX849, levels of active GTP-bound KRAS were maintained in KRAS$^{G12C/Y96D}$-expressing cells (Fig. 3E; ref. 22). These results suggest that the KRAS^{Y96D} mutation disrupts KRAS^{G12C} inhibitor binding, leading to sustained KRAS signaling and therapeutic resistance.

The Active State KRAS^{G12C} Inhibitor RM-018 Overcomes KRAS$^{G12C/Y96D}$

As KRAS$^{G12C/Y96D}$ conferred resistance to multiple KRAS^{G12C} inhibitors currently in clinical development, suggestive of shared vulnerability for this class of inhibitors, we sought to identify whether a structurally and functionally distinct KRAS^{G12C} inhibitor might retain potency against this resistance mutation. RM-018 is a novel KRAS^{G12C} inhibitor that binds specifically to the GTP-bound, active ["RAS(ON)"] state of KRAS^{G12C}. RM-018 is a "tricomplex" KRAS inhibitor, which exploits a highly abundant chaperone protein, cyclophilin A, to bind and inhibit KRAS^{G12C}, as previously described (Fig. 4A; structure shown in Supplementary Fig. S5; refs. 23, 24). Briefly, upon entering the cell, RM-018 forms a "binary complex" with cyclophilin A. This binary complex can associate with the active state of KRAS^{G12C}, aided by protein–protein surface interactions between cyclophilin A and KRAS, and forms a covalent bond with KRAS^{G12C} in a mutant-selective manner. This resultant "tricomplex" inhibits KRAS^{G12C} through binding of cyclophilin A, leading to steric occlusion and preventing the association of downstream effector proteins. Given the markedly different mechanism of action of this class of inhibitor, we hypothesized that the inhibitory activity of RM-018 might be differentially affected by KRAS^{Y96D} compared with inactive-state KRAS^{G12C} inhibitors.

RM-018 demonstrated selectivity for KRAS^{G12C}-driven cells, exhibiting low nanomolar potency in *KRAS*^{G12C}-mutant H358 cells while not impairing the viability of cells driven by KRAS^{G12D}, BRAF^{V600E}, or RTK-driven signaling through wild-type RAS (Fig. 4B). Interestingly, although KRAS$^{G12C/Y96D}$ expression led to marked IC_{50} shifts of >100-fold for

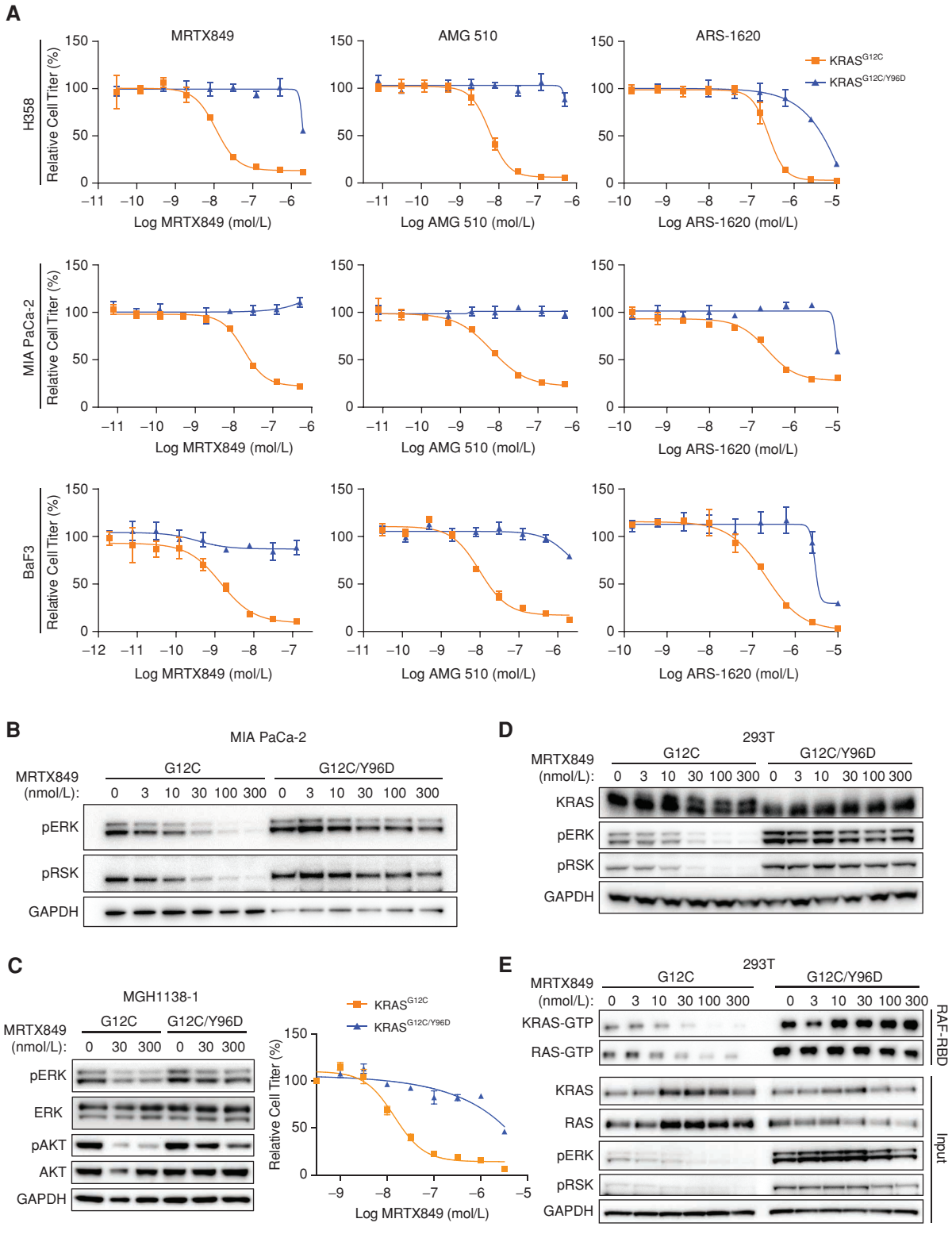

Figure 3. Cellular characterization of KRAS^{Y96D} in KRAS^{G12C}-mutant models. **A,** Cell viability assays performed with NCI-H358, MIA PaCa-2, and Ba/F3 cells infected with retrovirus packaging *KRAS* (G12C or G12C/Y96D). Cell lines were treated with indicated drugs for 72 hours and the viabilities were measured with CellTiter-Glo. **B,** Western blot analysis was performed after treating MIA PaCa-2 cells stably expressing KRAS^{G12C} or KRAS$^{G12C/Y96D}$ with MRTX849 for 4 hours. **C,** MGH1138-1 cells expressing KRAS^{G12C} or KRAS$^{G12C/Y96D}$ were treated with MRTX849 for 4 hours and subjected to Western blot analysis (left) and cell viability assay following 72 hours of treatment with the indicated concentrations of MRTX849 (right). **D,** Western blot analysis of HEK293T cells transiently expressing KRAS mutants after treatment with MRTX849 for 4 hours. **E,** RAS-GTP pulldown was performed after treating HEK293T stably expressing KRAS mutants with MRTX849.

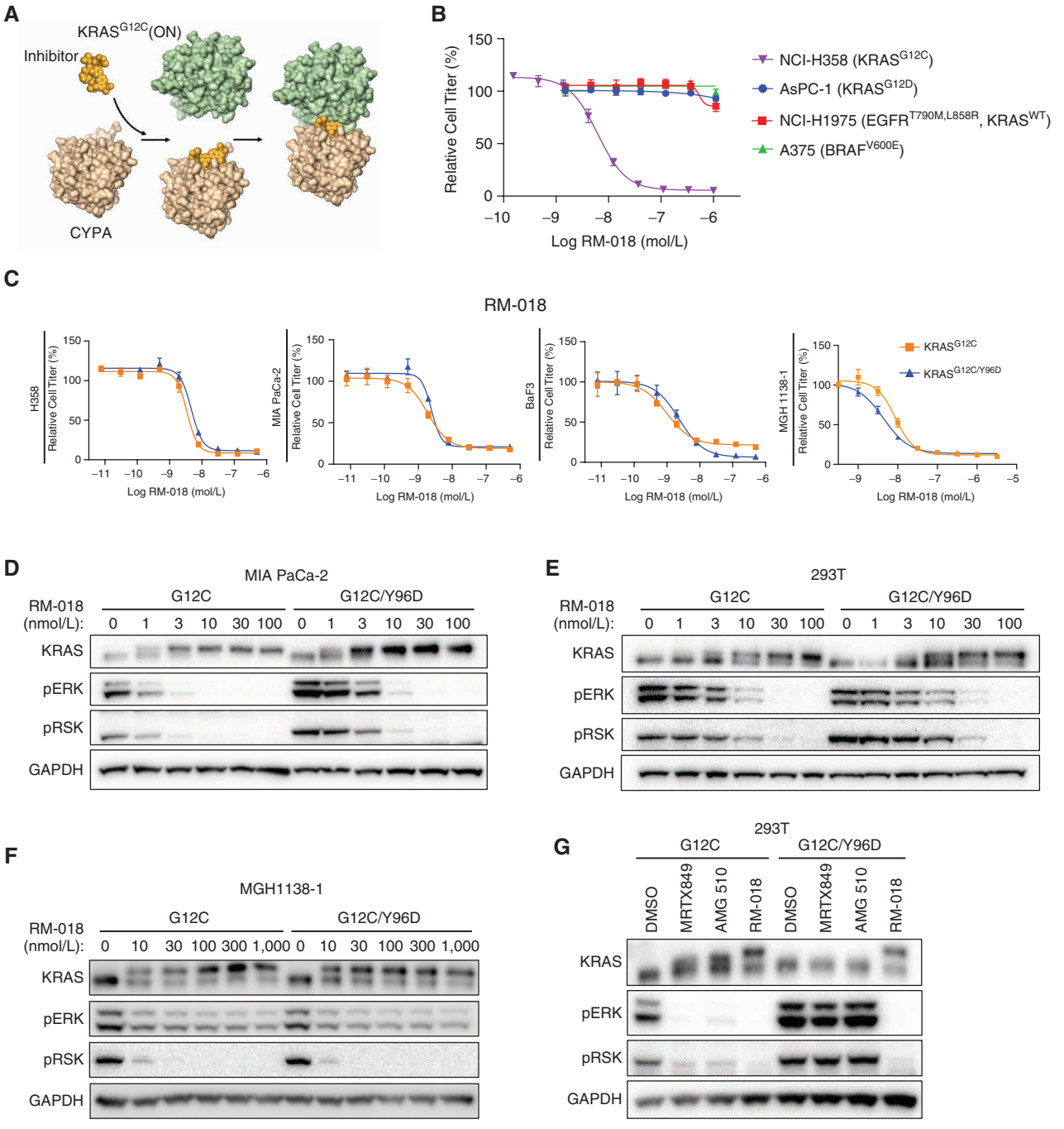

Figure 4. Novel KRAS inhibitor RM-018 overcomes KRAS$^{G12C/Y96D}$. **A,** Mechanism of action of RM-018. **B,** RM-018 selectively inhibits cell viability in cells harboring KRAS^{G12C}. **C,** Cell viability assays performed with NCI-H358, MIA PaCa-2, Ba/F3, and MGH1138-1 cells stably infected with KRAS^{G12C} or KRAS$^{G12C/Y96D}$ treated for 72 hours with RM-018. **D** and **E,** Western blot analysis performed in MIA PaCa-2 stably expressing KRAS^{G12C} or KRAS$^{G12C/Y96D}$ (**D**) and HEK293T cells transiently expressing KRAS mutants (**E**) after treatment of RM-018 for 4 hours. **F,** Western blot analysis of MGH1138-1 cells transiently expressing KRAS^{G12C} or KRAS$^{G12C/Y96D}$ after treatment with RM-018 for 4 hours. **G,** HEK293T cells transiently expressing KRAS mutants were treated with the indicated drug at 100 nmol/L each for 4 hours and then subjected to Western blot analysis.

MRTX849 and AMG 510 and ~20-fold for ARS-1620 (Fig. 3A) relative to KRAS^{G12C} expression alone, the efficacy of RM-018 on cell viability was largely unaffected by KRAS$^{G12C/Y96D}$ expression, with IC_{50} shifts of only ~2-fold (Fig. 4C; Supplementary Table S4). In addition, RM-018 was able to inhibit pERK and pRSK levels with similar potency in the presence of KRAS^{G12C} or KRAS$^{G12C/Y96D}$ expression in MIA PaCa-2, 293T cells, and the patient-derived *KRAS*^{G12C}-mutant NSCLC cell line MGH1138-1 (Fig. 4D–F). Inhibition of cell viability by RM-018 was also unaffected by KRAS$^{G12C/Y96D}$

expression in the patient-derived MGH1138-1 model. Furthermore, the KRAS mobility shift induced by covalent binding of RM-018 was observed in both cell lines in the presence of either KRAS^{G12C} or KRAS$^{G12C/Y96D}$ expression, suggesting that binding of RM-018 to KRAS is not abrogated by the KRAS^{Y96D} mutation. Indeed, although a KRAS mobility shift due to covalent drug binding was observed in 293T cells expressing KRAS^{G12C} for MRTX849, AMG 510, and RM-018, only RM-018 exhibited this same mobility shift and was able to inhibit downstream signaling in the presence of the KRAS$^{G12C/Y96D}$ mutation (Fig. 4G). Taken together, these data suggest that RM-018 retains the ability to bind and inhibit KRAS$^{G12C/Y96D}$ and may represent a potential therapeutic strategy to overcome this acquired resistance mechanism.

DISCUSSION

The arrival of covalent KRAS^{G12C}-selective inhibitors in the clinic and early signs of activity demonstrated by MRTX849 and AMG 510 have generated great enthusiasm (4, 5). However, our experiences across targeted therapies in lung cancer and other cancers collectively demonstrate that acquired resistance to the KRAS^{G12C} inhibitors will represent an inevitable challenge going forward. Although preclinical studies have nominated putative mechanisms of up-front resistance, including RAS–MAPK pathway reactivation (4, 8), mechanisms of acquired resistance to MRTX849 or AMG 510 causing disease relapse in patients remain unknown.

The acquired resistance demonstrated in this patient is instructive in highlighting several points. First, 10 distinct resistance alterations arose in this patient, all converging on the reactivation of RAS–MAPK signaling, suggesting that this may be a central common mechanism of acquired resistance. RAS reactivation occurred by multiple different mechanisms, including (i) activation of another RAS isoform (in this case, *NRAS*); (ii) other *KRAS* activating mutations in *trans* (G13D, G12V); (iii) potential loss of *KRAS*^{G12C} through a mutational switch to a different *KRAS* mutation in *cis*, although supported by limited sequencing reads; and (iv) a novel secondary alteration in *KRAS* (i.e., Y96D), which alters inhibitor binding.

Structural modeling predicted that this *KRAS*^{Y96D} mutation disrupts critical hydrogen bonding between the Y96 residue of KRAS and MRTX849. Importantly, we found that this *KRAS*^{Y96D} mutation conferred resistance not only to MRTX849 but also to additional KRAS^{G12C}-selective inhibitors in clinical development, AMG 510 and ARS-1620, highlighting that mutations affecting the Y96 residue of KRAS may represent a shared vulnerability for the currently available KRAS^{G12C} inhibitors. Continued investigation into clinical mechanisms of resistance to KRAS^{G12C} inhibitors in larger cohorts of patients will be required to define the spectrum and frequency of KRAS^{Y96} mutations (as well as other on-target mutations). Nonetheless, in light of our observations, it may be necessary to develop novel compounds that are able to target KRAS$^{G12C/Y96D}$ to overcome resistance to KRAS^{G12C} inhibitors in clinic. RM-018 was identified as a novel KRAS^{G12C} inhibitor with a distinct mechanism of action for targeting KRAS, which was uniquely able to overcome KRAS$^{G12C/Y96D}$ across multiple models. These results suggest that a novel, distinct KRAS inhibitor could theoretically be used to target resistance after an acquired *KRAS* resistance mutation emerges on the initial KRAS^{G12C} inhibitor, and they support efforts toward rational design of next-generation inhibitors.

Of note, however, the abundance of mutations downstream of RAS suggests that MAPK reactivation alone may be sufficient to drive resistance in at least some KRAS^{G12C} cancers. At the time of disease progression on MRTX849, this patient's plasma biopsy specimen revealed a low allele fraction of *KRAS*^{Y96D}, particularly compared with the significantly higher allele fraction of *KRAS*^{G12C} (0.4% vs. 31.7%, respectively), suggestive of the presence of polyclonal resistance to MRTX849 (with KRAS$^{G12C/Y96D}$-harboring tumor cells representing a minor subclone). Concordant with this notion and prior reports based on preclinical models, subsequent posttreatment plasma samples in this case revealed numerous mutations affecting various nodes of the RAS–MAPK pathway (including *NRAS, BRAF*, and *MAP2K1* mutations). Thus, rational combinations of KRAS^{G12C} inhibitors with downstream MAPK pathway inhibitors may be needed to successfully prevent or overcome resistance. Although analysis of additional patients is clearly needed to more fully define the spectrum of potential acquired resistance mechanisms to KRAS^{G12C} inhibitors, this study begins to delineate some of the potential resistance alterations that may be observed clinically. Ultimately, an iterative discovery process of identifying mechanisms of resistance and validating *in vitro* with a detailed structural and molecular understanding should help advance the development of novel strategies for therapeutic targeting of *KRAS*-mutant cancers.

METHODS

Patient Treatment and Specimen Collection

The patient was treated with MRTX849 dosed 600 mg twice daily on the phase I study (KRYSTAL-1) after providing written informed consent (ClinicalTrials.gov identifier: NCT03785249). She had received two prior lines of therapy. All pre- and posttreatment biopsies and genotyping were performed in accordance with the Massachusetts General Hospital (MGH) institutional review board–approved protocol and in accordance with the Declaration of Helsinki. The pretreatment tumor specimen was analyzed using the MGH SNaPshot next-generation sequencing assay (25). All cfDNA samples were sequenced using the commercially available Guardant360 assay (Guardant Health). More detailed patient history is available in the Supplement.

Cell Lines and Reagents

Ba/F3 cells were obtained from the RIKEN BRC Cell Bank (RIKEN BioResource Center). MGH1138-1 cells were generated from a patient with *KRAS*^{G12C}-mutant NSCLC using methods that have been previously described (26). Prior to cell line generation, the patient provided written informed consent to participate in a Dana-Farber/Harvard Cancer Center institutional review board–approved protocol giving permission for research to be performed on their sample. The remaining cell lines were obtained from ATCC or the Center for Molecular Therapeutics at the MGH Cancer Center, which routinely performs cell line authentication testing by SNP and short-tandem repeat analysis. HEK293T cells were maintained in DMEM supplemented with 10% FBS. MIA PaCa-2 and NCI-H358 cells were maintained in DMEM/F12 supplemented with 10% FBS. LU-65 and MGH1138-1 cells were maintained in RPMI supplemented with 10% FBS. Ba/F3 cells were maintained in DMEM supplemented

with 10% FBS and 10 ng/mL IL3. The *KRAS* (G12C or G12C/Y96D) gene was inserted in pMXs-Puro Retroviral Expression Vector, which was purchased from Cell Biolabs. Retrovirus packaging mutated *KRAS* genes were produced with HEK293T cells. After concentration of virus with Retro-Concentin Retro Concentration Reagent (System Biosciences), MIA PaCa-2, NCI-H358, and Ba/F3 cells were infected with the virus packaging either the $KRAS^{G12C}$ or $KRAS^{G12C/Y96D}$ gene. After 48 hours of incubation, the cells were treated with puromycin (1–2 μg/mL) for another 48 hours. IL3 was withdrawn to select for Ba/F3 cells dependent on mutant KRAS signaling after 48 hours of puromycin treatment. The remaining cells were maintained in media supplemented with puromycin. For transient expression experiments, a day after seeding the cells, pMXs-Puro-$KRAS^{G12C}$ or pMXs-Puro-$KRAS^{G12C/Y96D}$ vectors were induced with Lipofectamine 2000 Transfection Reagent (ThermoFisher Scientific) following the manufacturer's protocol. After 16 to 24 hours of incubation, cells were treated with inhibitors for 4 hours. AMG 510 was purchased from MedChemExpress. MRTX849 and ARS-1620 were purchased from Selleck Chemicals. RM-018 was provided by Revolution Medicines, and details of the chemical synthesis can be found in International Patent Application No. PCT/US2020/058841.

Cell Viability Assays

Cell lines were seeded in a 96-well plate at 2 to 10×10^3 cells/well depending on cell lines and after 24 hours treated with a serial dilution of drugs and incubated for 72 hours. Cell viability was measured with CellTiter-Glo (Promega).

Western Blot Analysis

Cell lines were treated with MRTX849, AMG 510, or RM-018 for 4 hours and lysates were prepared as described previously (27). All antibodies were diluted in 5% bovine serum albumin as follows: KRAS (Sigma), pERK (Thr202/Tyr204,1:1,000; Cell Signaling Technology), p44/42 MAPK (ERK1/2) (1:1,000; Cell Signaling Technology), phospho-RSK1 (T359+S363, 1:1,000; Abcam), phospho-AKT (Ser473, 1:1,000; Cell Signaling Technology), AKT (1:1,000; Cell Signaling Technology), and GAPDH (1:1,000; MilliporeSigma).

RAS-GTP Pulldown

After indicated inhibitor treatment, RAS activity was assessed by GST-RAF-RBD pulldown (Cell Signaling Technology), followed by Western blot analysis with pan-RAS or RAS isoform–specific antibodies. Pulldown samples and whole-cell lysates were resolved on 4% to 12% Bis-Tris gels, and Western blotting was performed using antibodies against KRAS (Sigma) and pan-RAS (Cell Signaling Technology).

Structural Modeling

Publicly available crystal structures of $KRAS^{G12C}$ in complex with MRTX849 (PDB:6UT0), AMG 510 (PDB:6OIM), and ARS-1620 (PDB:5V9U) were downloaded from the RCSB Protein Data Bank (PDB; ref. 28). Structures were rendered in PyMol (The PyMOL Molecular Graphics System) and analyzed for hydrogen bonds and other molecular interactions between the $KRAS^{G12C}$ inhibitors and the KRAS protein. Structures of Y96 amino acid mutation were generated by Protein Mutagenesis Wizard implemented in PyMol, with one of the backbone-dependent rotamers manually selected.

cfDNA Extraction and ddPCR

Whole blood was collected by routine phlebotomy in two 10-mL Streck tubes. Plasma was separated within 1 to 4 days of collection through two different centrifugation steps (the first at room temperature for 10 minutes at $1,600 \times g$ and the second at $3,000 \times g$ for the same time and temperature). Plasma was stored at −80°C until cfDNA extraction. cfDNA was extracted from plasma using the QIAamp Circulating Nucleic Acid Kit (QIAGEN) with 60 minutes of proteinase K incubation at 60°C. All other steps were performed according to the manufacturer's instructions. For ddPCR experiments, DNA template (up to 10 μL, with a total of 20 ng) was added to 12.5 μL ddPCR Supermix for Probes (Bio-Rad) and 1.25 μL custom primer/probe mixture. This reaction mix was added to a DG8 cartridge together with 60 μL Droplet Generation Oil for Probes (Bio-Rad) and used for droplet generation. Droplets were then transferred to a 96-well plate (Eppendorf) and then thermal cycled with the following conditions: 5 minutes at 95°C, 40 cycles of 94°C for 30 seconds, 55°C (with a few grades of difference among assays) for 1 minute, followed by 98°C for 10 minutes (Ramp Rate 2°C/s). Droplets were analyzed with the QX200 Droplet Reader (Bio-Rad) for fluorescent measurement of FAM and HEX probes. Gating was performed based on positive and negative controls, and mutant populations were identified. The ddPCR data were analyzed with QuantaSoft analysis software (Bio-Rad) to obtain fractional abundance of the mutant DNA alleles in the wild-type/normal background. The quantification of the target molecule was presented as the number of total copies (mutant plus wild-type) per sample in each reaction. Allelic fraction was calculated as follows: AF % = $[N_{mut}/(N_{mut} + N_{wt}) * 100]$, where N_{mut} is the number of mutant alleles and N_{wt} is the number of wild-type alleles per reaction. ddPCR analysis of normal control plasma DNA (from cell lines) and no DNA template controls was always included. Probe and primer sequences are available upon request.

Authors' Disclosures

N. Tanaka reports other support from Japanese Foundation for Cancer Research during the conduct of the study. J.J. Lin reports personal fees and other support from Genentech, personal fees from C4 Therapeutics, personal fees from Nuvalent, personal fees from Blueprint Medicines, personal fees and other support from Turning Point Therapeutics, personal fees and other support from Elevation Oncology, personal fees from Pfizer, other support from Hengrui Therapeutics, other support from Novartis, other support from Neon Therapeutics, other support from Relay Therapeutics, other support from Bayer, and other support from Roche outside the submitted work. L.A. Kiedrowski reports other support from Guardant Health during the conduct of the study. D. Juric reports grants and personal fees from Novartis, grants and personal fees from Genentech, grants and personal fees from EMD Serono, grants and personal fees from Eisai, personal fees from Guardant, personal fees from Ipsen, personal fees from Petra Pharma, personal fees from Mapkure, personal fees from Vibliome, personal fees from Relay Therapeutics, grants from Takeda, grants and personal fees from Syros, grants from Ribon Therapeutics, grants from Infinity Pharmaceuticals, grants from InventisBio, and grants from Amgen outside the submitted work. J.F. Gainor reports personal fees from Mirati and personal fees from Amgen during the conduct of the study, personal fees from Bristol-Myers Squibb, personal fees from Genentech/Roche, personal fees from Takeda, personal fees from Lilly, personal fees and other support from Blueprint, personal fees from Oncorus, personal fees from Regeneron, personal fees from Gilead, personal fees from AstraZeneca, personal fees from Pfizer, grants and personal fees from Novartis, personal fees and other support from Merck, personal fees from Agios, other support from Moderna, other support from Jounce, other support from Array, other support from Alexo outside the submitted work, and an immediate family member who is an employee with equity at Ironwood Pharmaceuticals. S.J. Klempner reports personal fees from BMS, personal fees from Merck, personal fees from Daiichi-Sankyo, personal fees from Astellas, personal fees from Pieris Oncology, personal fees from Natera, personal fees from Foundation Medicine, and other support from Turning Point Therapeutics outside the submitted work. L. Bar-Peled reports personal fees from Scorpion

Therapeutics outside the submitted work. A.N. Hata reports grants from Amgen, grants from Eli Lilly, grants from Relay Therapeutics, grants from Roche/Genentech, grants from Novartis, grants from Blueprint Medicines, grants from Pfizer, and grants and personal fees from Nuvalent outside the submitted work. R.S. Heist reports personal fees from Novartis, personal fees from Daichii Sankyo, personal fees from EMD Serono, personal fees from Tarveda, personal fees from Apollomics, grants from Novartis, grants from Corvus, grants from Incyte, grants from Genentech Roche, grants from Mirati, grants from Turning Point, grants from BMS, grants from Daichii Sankyo, grants from AbbVie, grants from Agios, grants from Exelixis, and grants from Lilly outside the submitted work. R.B. Corcoran reports personal fees from AbbVie, grants and personal fees from Asana Biosciences, personal fees from Astex Pharmaceuticals, grants and personal fees from AstraZeneca, personal fees and other support from Avidity Biosciences, personal fees and other support from C4 Therapeutics, personal fees from Chugai, personal fees from Elicio, other support from Erasca, personal fees from Fog Pharma, personal fees from Guardant Health, personal fees from Ipsen, personal fees and other support from Kinnate Biopharma, personal fees from Mirati Therapeutics, personal fees from Natera, grants from Novartis, grants from Lilly, personal fees and other support from nRichDx, personal fees from Pfizer, personal fees from QIAGEN, personal fees and other support from Remix Therapeutics, personal fees and other support from Revolution Medicines, personal fees from Roivant, personal fees from Shionogi, personal fees from Tango Therapeutics, personal fees from Taiho, and personal fees from Zikani Therapeutics outside the submitted work; in addition, R.B. Corcoran has a patent for Intellectual Property pending. No disclosures were reported by the other authors.

Authors' Contributions

N. Tanaka: Conceptualization, data curation, formal analysis, investigation, writing–original draft, writing–review and editing. **J.J. Lin:** Conceptualization, data curation, formal analysis, investigation, writing–original draft, writing–review and editing. **C. Li:** Conceptualization, data curation, formal analysis, investigation, writing–original draft, writing–review and editing. **M.B. Ryan:** Conceptualization, data curation, formal analysis, investigation, writing–original draft, writing–review and editing. **J. Zhang:** Conceptualization, formal analysis, writing–original draft, writing–review and editing. **L.A. Kiedrowski:** Conceptualization, formal analysis, writing–review and editing. **A.G. Michel:** Formal analysis, investigation, writing–review and editing. **M.U. Syed:** Formal analysis, investigation, writing–review and editing. **K.A. Fella:** Formal analysis, investigation, writing–review and editing. **M. Sakhi:** Formal analysis, investigation, writing–review and editing. **I. Baiev:** Formal analysis, investigation, writing–review and editing. **D. Juric:** Conceptualization, formal analysis, investigation, writing–review and editing. **J.F. Gainor:** Conceptualization, formal analysis, investigation, writing–review and editing. **S.J. Klempner:** Conceptualization, formal analysis, investigation, writing–review and editing. **J.K. Lennerz:** Formal analysis, investigation, writing–review and editing. **G. Siravegna:** Conceptualization, data curation, formal analysis, supervision, investigation, writing–original draft, writing–review and editing. **L. Bar-Peled:** Conceptualization, data curation, formal analysis, supervision, investigation, writing–review and editing. **A.N. Hata:** Conceptualization, resources, data curation, formal analysis, supervision, funding acquisition, validation, investigation, writing–original draft, writing–review and editing. **R.S. Heist:** Conceptualization, resources, data curation, formal analysis, supervision, funding acquisition, validation, investigation, writing–original draft, writing–review and editing. **R.B. Corcoran:** Conceptualization, resources, data curation, formal analysis, supervision, funding acquisition, validation, investigation, writing–original draft, writing–review and editing.

Acknowledgments

RM-018 was kindly provided by Revolution Medicines. This research was supported in part by a Mark Foundation for Cancer Research EXTOL Project Grant (J.F. Gainor, A.N. Hata) and a Stand Up To Cancer—American Cancer Society Lung Cancer Dream Team Translational Research Grant (J.F. Gainor, A.N. Hata; grant number: SU2C-AACR-DT17–15). Stand Up To Cancer (SU2C) is a division of the Entertainment Industry Foundation. The indicated SU2C research grant is administered by the American Association for Cancer Research, a scientific partner of SU2C. J.J. Lin is partially supported by funding from NIH R01-CA164273. C. Li is supported by funding from NIH 1F32CA250231–01. N. Tanaka is partially supported by funding from US-JFCR Scientist Exchange Program. L. Bar-Peled is supported by AACR (19–20–45-BARP), Damon Runyon (DRR-62–20), and NIH/NCI (R00 CA215249).

Received March 19, 2021; revised March 30, 2021; accepted April 1, 2021; published first April 6, 2021.

REFERENCES

1. Fell JB, Fischer JP, Baer BR, Blake JF, Bouhana K, Briere DM, et al. Identification of the clinical development candidate MRTX849, a covalent KRAS(G12C) inhibitor for the treatment of cancer. J Med Chem 2020;63:6679–93.
2. Lanman BA, Allen JR, Allen JG, Amegadzie AK, Ashton KS, Booker SK, et al. Discovery of a covalent inhibitor of KRAS(G12C) (AMG 510) for the treatment of solid tumors. J Med Chem 2020;63:52–65.
3. Ostrem JM, Peters U, Sos ML, Wells JA, Shokat KM. K-Ras(G12C) inhibitors allosterically control GTP affinity and effector interactions. Nature 2013;503:548–51.
4. Hallin J, Engstrom LD, Hargis L, Calinisan A, Aranda R, Briere DM, et al. The KRAS(G12C) inhibitor MRTX849 provides insight toward therapeutic susceptibility of KRAS-mutant cancers in mouse models and patients. Cancer Discov 2020;10:54–71.
5. Hong DS, Fakih MG, Strickler JH, Desai J, Durm GA, Shapiro GI, et al. KRAS(G12C) inhibition with sotorasib in advanced solid tumors. N Engl J Med 2020;383:1207–17.
6. Li B, Skoulidis F, Falchook G, Sacher A, Velcheti V, Dy G, et al. PS01.07 registrational phase 2 trial of sotorasib in KRAS p.G12C mutant NSCLC: first disclosure of the codebreak 100 primary analysis. J Thorac Oncol 2021;16:S61.
7. Jänne PA, Rybkin II, Spira AI, Riely GJ, Papadopoulos KP, Sabari JK, et al. KRYSTAL-1: activity and safety of adagrasib (MRTX849) in advanced/metastatic non–small-cell lung cancer (NSCLC) harboring KRAS G12C mutation. Eur J Cancer 2020;138:S1–S2.
8. Ryan MB, Fece de la Cruz F, Phat S, Myers DT, Wong E, Shahzade HA, et al. Vertical pathway inhibition overcomes adaptive feedback resistance to KRAS(G12C) inhibition. Clin Cancer Res 2020;26:1633–43.
9. Misale S, Fatherree JP, Cortez E, Li C, Bilton S, Timonina D, et al. KRAS G12C NSCLC models are sensitive to direct targeting of KRAS in combination with PI3K inhibition. Clin Cancer Res 2019;25:796–807.
10. Santana-Codina N, Chandhoke AS, Yu Q, Malachowska B, Kuljanin M, Gikandi A, et al. Defining and targeting adaptations to oncogenic KRAS(G12C) inhibition using quantitative temporal proteomics. Cell Rep 2020;30:4584–99.
11. Solanki HS, Welsh EA, Fang B, Izumi V, Darville L, Stone B, et al. Cell type-specific adaptive signaling responses to KRAS(G12C) inhibition. Clin Cancer Res 2021;27:2533–48.
12. Xue JY, Zhao Y, Aronowitz J, Mai TT, Vides A, Qeriqi B, et al. Rapid non-uniform adaptation to conformation-specific KRAS(G12C) inhibition. Nature 2020;577:421–5.
13. Fedele C, Li S, Teng KW, Foster CJR, Peng D, Ran H, et al. SHP2 inhibition diminishes KRASG12C cycling and promotes tumor microenvironment remodeling. J Exp Med 2021;218:e20201414.
14. Kinoshita-Kikuta E, Kinoshita E, Ueda S, Ino Y, Kimura Y, Hirano H, et al. Increase in constitutively active MEK1 species by introduction

of MEK1 mutations identified in cancers. Biochim Biophys Acta Proteins Proteom 2019;1867:62–70.
15. Gao Y, Chang MT, McKay D, Na N, Zhou B, Yaeger R, et al. Allele-specific mechanisms of activation of MEK1 mutants determine their properties. Cancer Discov 2018;8:648–61.
16. Canon J, Rex K, Saiki AY, Mohr C, Cooke K, Bagal D, et al. The clinical KRAS(G12C) inhibitor AMG 510 drives anti-tumour immunity. Nature 2019;575:217–23.
17. Sondka Z, Bamford S, Cole CG, Ward SA, Dunham I, Forbes SA. The COSMIC Cancer Gene Census: describing genetic dysfunction across all human cancers. Nat Rev Cancer 2018;18:696–705.
18. Consortium APG. AACR Project GENIE: powering precision medicine through an international consortium. Cancer Discov 2017;7:818–31.
19. Fell JB, Fischer JP, Baer BR, Ballard J, Blake JF, Bouhana K, et al. Discovery of tetrahydropyridopyrimidines as irreversible covalent inhibitors of KRAS-G12C with in vivo activity. ACS Med Chem Lett 2018;9:1230–4.
20. Janes MR, Zhang J, Li LS, Hansen R, Peters U, Guo X, et al. Targeting KRAS mutant cancers with a covalent G12C-specific inhibitor. Cell 2018;172:578–89.
21. Chen H, Smaill JB, Liu T, Ding K, Lu X. Small-molecule inhibitors directly targeting KRAS as anticancer therapeutics. J Med Chem 2020;63:14404–24.
22. Zeng M, Lu J, Li L, Feru F, Quan C, Gero TW, et al. Potent and selective covalent quinazoline inhibitors of KRAS G12C. Cell Chem Biol 2017;24:1005–16.
23. Schulze CJ, Bermingham A, Choy TJ, Cregg JJ, Kiss G, Marquez A, et al. Abstract PR10: tri-complex inhibitors of the oncogenic, GTP-bound form of $KRAS^{G12C}$ overcome RTK-mediated escape mechanisms and drive tumor regressions in vivo. Mol Cancer Ther 2019;18:PR10.
24. Nichols R, Schulze C, Bermingham A, Choy T, Cregg J, Kiss G, et al. A06 Tri-complex inhibitors of the oncogenic, GTP-bound form of KRASG12C overcome RTK-mediated escape mechanisms and drive tumor regressions in preclinical models of NSCLC. J Thorac Oncol 2020;15:S13–S4.
25. Zheng Z, Liebers M, Zhelyazkova B, Cao Y, Panditi D, Lynch KD, et al. Anchored multiplex PCR for targeted next-generation sequencing. Nat Med 2014;20:1479–84.
26. Crystal AS, Shaw AT, Sequist LV, Friboulet L, Niederst MJ, Lockerman EL, et al. Patient-derived models of acquired resistance can identify effective drug combinations for cancer. Science 2014;346:1480–6.
27. Ahronian LG, Sennott EM, Van Allen EM, Wagle N, Kwak EL, Faris JE, et al. Clinical acquired resistance to RAF inhibitor combinations in BRAF-mutant colorectal cancer through MAPK pathway alterations. Cancer Discov 2015;5:358–67.
28. Berman HM, Westbrook J, Feng Z, Gilliland G, Bhat TN, Weissig H, et al. The protein data bank. Nucleic Acids Res 2000;28:235–42.